Numerical modeling and experimental analysis of the magnetic noise of the single-phase, inverter-fed permanent split-capacitor motor

Andrei NEGOITA[1], Gheorghe SCUTARU[1], Ioan PETER[2], Razvan Mihai IONESCU[1], Ovidiu PLESA[1], Ciprian NISTOR[1]
"Transilvania" University of Brasov, Romania, S.C. "Electroprecizia" S.A. Brasov, Romania
E-mail : andrei.negoita@yahoo.com; scutaru@unitbv.ro, ioan.peter@electroprecizia.ro

***Abstract*- The paper presents a FEM approach for studying the influence of the capacitor value on the magnetic noise of a network and inverter-fed permanent split-capacitor induction motor. A 4 pole, 24 stator slots and 30 rotor slots, induction motor is modeled under Flux2D Finite Element software in order to determine the amplitude and frequency spectrum of the magnetic forces acting on the stator. The effects of the inverter supply are taken into account by coupling Flux2D with Matlab/Simulink. The results are compared with those obtained from noise measurements performed on the studied motor.**

I. INTRODUCTION

Single phase induction motors are widely used in many household and industrial applications. Thus, noise and vibrations standard compliance is a primary requirement for any such device.

From the motor designer point of view, new and accurate techniques are needed for motor design while taking into account the noise and vibration standard compliance. The Finite Element Methods (FEM) are well suited for such a purpose because they offer a high accuracy by taking into account the skin effect, the non-linearity and the changing of parameters with load [1].

The most common form of the single-phase machine is the permanent split-capacitor motor. [2], [3], shown in Figure 1.

Based on the revolving field theory, the analysis of the single phase induction motors has to take into account that:

- the revolving magnetic field is elliptic, being produced by a asymmetric double phase winding;

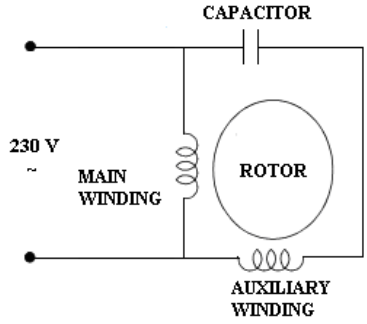

Fig. 1. The permanent split-capacitor motor supplied from the AC grid.

- two revolving magnetic waveforms, a direct and an inverse one, act in the machine;
- the phase angle between the currents of the main and auxiliary winding is achieved by placing a permanently connected capacitor in series with the auxiliary winding; the revolving magnetic field has a variable speed with time [3] and is circular only at startup, because the capacitor is usually calculated as to assure maximum motor performance in this regime;
- as a consequence of the elliptic magnetic field, a number of supplementary radial magnetic forces appear leading to noise and vibration;
- the optimum capacitance value is dependent on the load, as well as on the amplitude and frequency of the supplying voltage, thus, the pulsating torque poses a permanent vibration and noise problem [4].

Nowadays most of the typical applications require variable speed control through the use of inverters. Inverter fed induction motors are known to be noisier than network fed ones because of the higher harmonic content of the supply current which leads to a higher probability of matching the exciting forces frequencies with natural stator frequencies [5].

The aim of the paper is to study the influence of the capacitor on the magnetic noise of the single-phase motor. To this end, a FEM approach was used for calculating the magnetic forces acting on the stator surface. In order to study the behavior of the inverter-fed motor, a method of coupling the Flux 2D motor model with a Matlab/Simulink inverter model is proposed.

The proposed model is validated by analyzing the noise-frequency characteristics obtained from testing a 0.75 kW, 1500 rpm, 4 pole, 24 stator slots and 30 rotor slots, permanent split-capacitor induction motor. The motor was tested in a semi-anechoic chamber according to the ISO 1680/1 standard. The test conditions were the following:

- network and inverter supply, nominal 50 Hz frequency; inverter switching frequency 4 kHz;
- no load operation;
- motor fitted in turn with three capacitors of 30 uF, 36 uF and 50 uF.

978-1-4673-1653-8/12/$31.00 ©2012 IEEE

II. INDUCTION MOTOR MODELING USING FLUX 2D

The motor geometry was constructed based on such parameters as: stator and rotor inner diameters, slot heights; slot top and bottom diameters and air-gap width.

The components needed for modeling each part of the motor have been defined in two separate coordinate systems, one attached to the stator and the other one attached to the rotor. This allows on one side, the accurate control of rotor bar position with respect to stator slot position and on the other side provides an easy way of controlling the alignment of the rotor with respect to the stator.

According to the description of the motor geometry, the model has 58 distinct regions accounting for the stator and rotor slots, stator core, airgap and motor shaft. Each region must be characterised both from electromagnetic and mechanical points of view.

For example, in order to fully define the regions occupied by the windings, one must define the type of region (stranded coil conductor), the direction of the current passing through that region (positive or negative), the material of the region and the mechanical set to which the region belongs to. In the case of the single phase, capacitor run, squirrel cage induction motor the two stator windings are placed ortogonally across the stator perifery as shown in Figure 2.

The numerical analysis of electrical devices is usually restricted by the complexity of the power supply. The field-circuit coupling allows the treating of electrical conductors and of their supply circuit by introducing the electrical equations directly into the magnetic field computation.

Figure 3 shows the electrical circuit constructed by using the specialised Electriflux circuit module of Flux 2D. In the following, a brief explanation of the circuit components corresponding to a capacitor run single phase induction motor which are defined in FLUX 2D is given :

1. a voltage source component defined, by the classical expression for a sinusoidal signal;
2. the two stator windings defined by using stranded conductors components for which the resistance of each phase is given
3. capacitor component used for creating the phase angle between the main and auxiliary winding currents
4. two resistances and inductances used for taking into account the front and back portions of the stator windings which are not modeled in the finite element domain and which have to be calculated based on such parameters as the number of stator slots, number of turns per slot per phase, number of slots per pole per phase and number of coils in parallel per phase [6]
5. Squirrel cage component for which the resistance and inductance of the portion between two adjacent rotor bars have to be calculated based on the dimensions of the end ring, rotor dimensions, the number of rotor slots and magnetic pole pair number

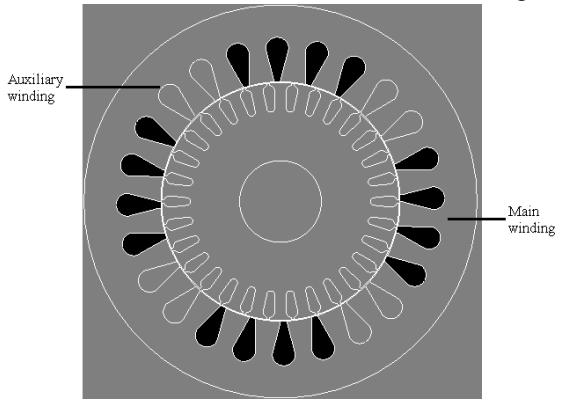

Fig. 2. Stator winding distribution.

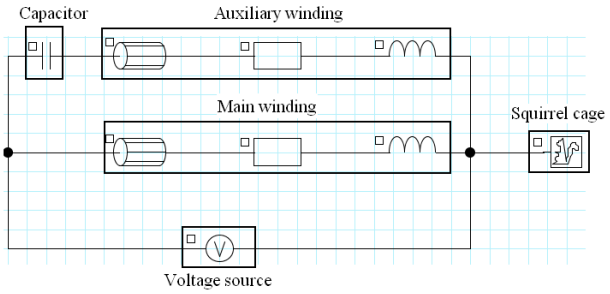

Fig. 3 Circuit topology for the studied motor.

In order to prove the validity of the proposed model, several characteristics are shown in figure 4, figure 5 and figure 6, accounting for the distribution of the magnetic field lines, the normal component of the air-gap flux density and the speed vs. time characteristics.

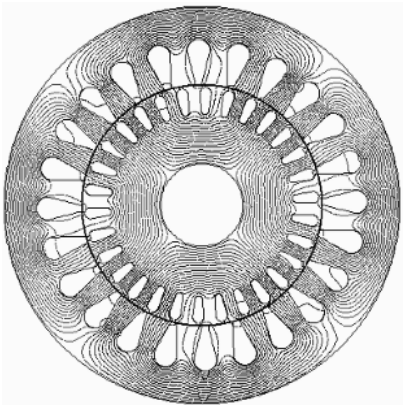

Fig. 4. Magnetic field lines.

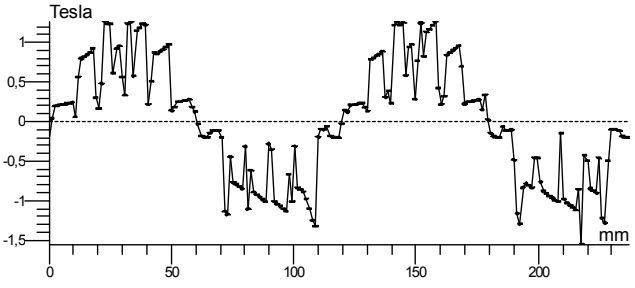

Fig. 5. Air-gap flux density (t=0.5 s).

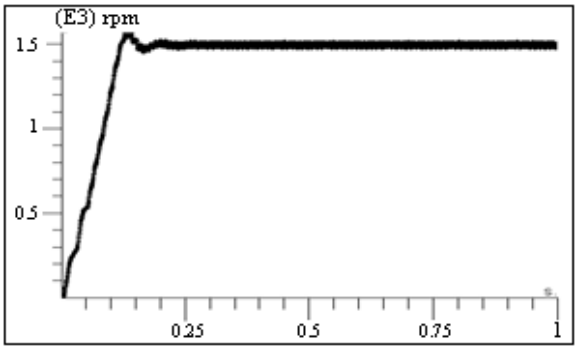

Fig. 6. Angular velocity vs. time.

III. NOISE AND VIBRATION CAUSES FOR INDUCTION MOTORS

In the case of induction motors, noise and vibration is caused by aerodynamic, mechanical and electromagnetic causes. From the electromagnetic point of view, there are four main causes that lead to magnetic flux density harmonics:

- magnetic saturation,
- presence of stator slots,
- higher time harmonics of the supply current,
- rotor eccentricity or machine asymmetries.

In the following, only the effects of the flux density harmonics caused by higher time harmonics of the supply current will be analyzed.

The analysis of the phenomenon that leads vibration and noise is more complex for inverter-fed induction motors.

Because of the increased air-gap flux density harmonic spectrum there is an increased possibility of matching the exciting frequencies of the magnetic forces with stator natural frequencies which leads to resonance, thus to excessive vibration and noise [5].

The stator current of an inverter-fed permanent split capacitor induction motor contains harmonics of the order:

$$n = 2k \pm 1; \quad k = 0, 1, 2, 3, \ldots \ . \tag{1}$$

In terms of Fourier series, the stator non-sinusoidal current can be expressed as [5]:

$$\begin{aligned} & i_1(t) = \sum_{n=1}^{\infty} \sqrt{2} I_{1,n} \sin\left(\omega_n t - \varphi_{1,n}\right); \\ & \omega_n = 2\pi n f; \\ & f_n = nf. \end{aligned} \tag{2}$$

The slip for the n^{th} harmonic is given by:

$$s_n = \frac{n \cdot n_s \mp n_s \cdot (1 - s)}{n \cdot n_s}, \tag{3}$$

in which:

$$n \cdot n_s = \frac{n \cdot f}{p}, \tag{4}$$

is the synchronous speed for the n^{th} harmonic, s is the slip for the fundamental harmonic.

For forward-rotating magnetic field:

$$\begin{aligned} & s_n = 1 - \frac{1 - s}{n}; \\ & \omega_n = n \omega s_n = \omega\left[1 - n(1 - s)\right]; \\ & s_{sn} = 1 - n. \end{aligned} \tag{5}$$

For backward-rotating magnetic field:

$$\begin{aligned} & s_n = 1 + \frac{1 - s}{n} \\ & \omega_n = n \omega s_n = \omega\left[1 + n(1 + s)\right] \\ & s_{sn} = 1 + n. \end{aligned} \tag{6}$$

As the induction motor operates at $s \le 0{,}05$, the slip for the n^{th} harmonic can be approximated as:

$$s_n \approx 1 \mp \frac{1}{n} \ . \tag{7}$$

By neglecting the tangential component of the magnetic flux density, according to the Maxwell stress tensor, the magnetic pressure waveform at any point of the air gap is:

$$p_r(\alpha, t) \approx \frac{{b_n}^2(\alpha, t)}{2\mu_0} = \frac{1}{2\mu_0}\left[b_1(\alpha, t) + b_2(\alpha, t)\right]^2 =$$

$$= \frac{1}{2\mu_0}\left\{\left[b_1(\alpha, t)\right]^2 + 2 b_1(\alpha, t)\, b_2(\alpha, t) + \left[b_2(\alpha, t)\right]^2\right\}. \tag{8}$$

In terms of Fourier series, the following three groups of magnetic pressure waves are produced:

- $p_{r\nu n}(\alpha, t)$ determined by the product $\left[b_1(\alpha, t)\right]^2$ of the stator harmonics of the same order ν:

$$p_{r\nu n}(\alpha, t) = \frac{B_{m\nu n}^2}{4\mu_0}\left[1 + \cos\left(2\nu\, p\, \alpha \mp 2\, \omega_n t\right)\right]. \tag{9}$$

For $\nu \ge 1$ and time harmonics $n \ge 1$, the frequency of the radial magnetic pressure is $f_{rn} = 2nf$ and the vibration mode $r = 2\nu p$.

- $p_{r\nu\mu n}(\alpha,t)$ determined by the mixed product $2b_1(\alpha,t)b_2(\alpha,t)$ of the stator harmonic ν and the rotor harmonic μ:

$$p_{r\nu\mu n}(\alpha,t)=\frac{1}{2\mu_0}\sum_{\nu=1}^{\infty}\sum_{\mu=1}^{\infty}B_{m\nu n}B_{m\mu n}$$
$$\{\cos[(\nu-\mu)p\alpha\mp(\omega_n-\omega_{\mu n})t-\phi_{\mu n}]+$$
$$+\cos[(\nu+\mu)p\alpha\mp(\omega_n+\omega_{\mu n})t+\phi_{\mu n}]\} \quad (10)$$

For $\nu\geq 1$, $\mu\geq 1$ and time harmonics $n\geq 1$, the frequency of the radial magnetic pressure is $f_{rn}=n(f\pm f_\mu)$ and the vibration mode $r=(\nu\pm\mu)p$.

- $p_{r\mu}(\alpha,t)$ determined by the product $[b_2(\alpha,t)]^2$ of the rotor harmonics of the same order μ:

$$p_{r\mu n}(\alpha,t)=\frac{B_{m\mu n}^2}{4\mu_0}[1+\cos(2\mu p\alpha\mp$$
$$\mp 2\omega_{\mu n}t+2\phi_{\mu n})]; \quad (11)$$

For $\mu\geq 1$ and time harmonics $n\geq 1$, the frequency of the radial magnetic pressure is $f_{rn}=2nf_\mu$ and the vibration mode $r=2\mu p$.

In addition, the following magnetic pressure waves are produced:

- Higher time stator harmonics of different numbers can produce significant radial forces [9] having the frequency $f_{r,n}=(n'\pm n'')f$; $n'\neq n''$ and the vibration mode $r=0$ or $r=2$. The most important are the magnetic forces due to sums and differences of the fundamental harmonic f with major higher time harmonics of the stator current:

$$f_{r,n}=(1\pm n)f \quad (12)$$

- The interaction of the switching frequency f_{sw} and higher time harmonics $f_n=n'f_{sw}\pm n''f$ produces large amplitude forces [5]. If n' is an odd integer, n'' will be an even integer and vice versa:

$$f_n=f_{sw}\pm 2f,$$
$$f_n=f_{sw}\pm 4f,$$
$$f_n=f_{sw}\pm 6f,\ldots \quad (13)$$

and

$$f_n=2f_{sw}\pm f,$$
$$f_n=2f_{sw}\pm 3f,$$
$$f_n=2f_{sw}\pm 5f,\ldots \quad (14)$$

The most important case is the interaction between the fundamental field harmonic and higher time harmonics:

$$f_{r,n}=|(\pm f_n)-f|, \quad (15)$$

and the vibration mode $r=0$.

- At full load and when force orders are low, interaction of the permeance field harmonics and MMF harmonics associated with higher time harmonics of the stator can produce important vibration [5]:

$$f_{r,n}=|(\pm f_n)-f|; \quad (16)$$

$$f_{r,n}=\left|f_n\pm f\left[1+k\frac{s_2}{p}(1-s)\right]\right|, \quad (17)$$

and the vibration mode $r=0,2$.

- Rectifier harmonics are transmitted to the stator winding via the intermediate circuit and inverter:

$$f_{r,n}=n,$$
$$f=2m_1kf, \quad (18)$$

where $k=1,2,3,\ldots$ and m_1 is the number of phases; the vibration mode $r=2p$.

IV. MATLAB/SIMULINK - FLUX2D COUPLING

The „FLUX2D-Coupling" block in Matlab Simulink enables the simulation of any 2D controlled electromagnetic device by controlling FLUX2D directly through the Simulink window. Simulink inputs and outputs are vectors of any dimension, generated by Mux or Demux blocks from a user-defined number of components. Any number of inputs and outputs can be defined to control and observe the modeled device or system. The Simulink to Flux 2D block accepts two types of quantities :

1. Electric : voltage, current, resistance, inductance;

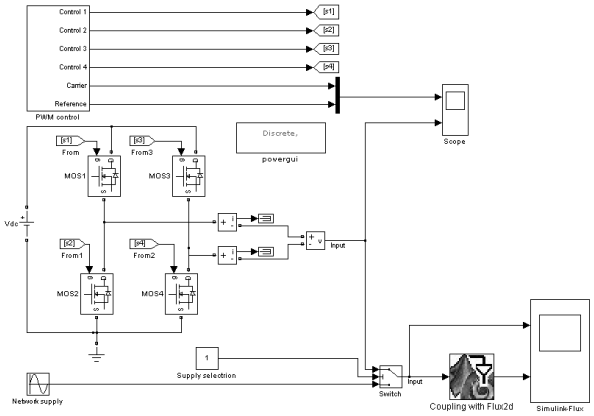

Fig. 7. Full bridge inverter - Simulink block diagram.

2. Mechanic :angular velocity, torque, inertia.

As shown in Figure 7, a full bridge inverter topology was used and a simple sine wave PWM control technique was implemented. The principle of the sine wave PWM technique is the generation of the desired output voltage achieved by comparing the desired reference waveform (modulating signal) with a high-frequency triangular 'carrier' wave.

The resulting square waveform contains a replica of the desired waveform in its low frequency components, with the higher frequency components being at frequencies of an close to the carrier frequency, in this case 4 kHz.

In order to show the validity of the Simulink inverter model, Figure 8 shows a comparison between the harmonic content of the supply current when the motor is network-fed and inverter-fed. As expected odd harmonics of orders n = 1, 3, 5, 7, 9 are present in the inverter-fed motor supply current spectrum [7]. The increased harmonic content of the supply current leads to an increased harmonic content of the air-gap flux density [8]:

$$b(\alpha,t) = F(\alpha,t) \cdot \Lambda(\alpha,t) \tag{19}$$

Figure 9, shows the influence of the inverter supply on the air-gap flux density spectrum.

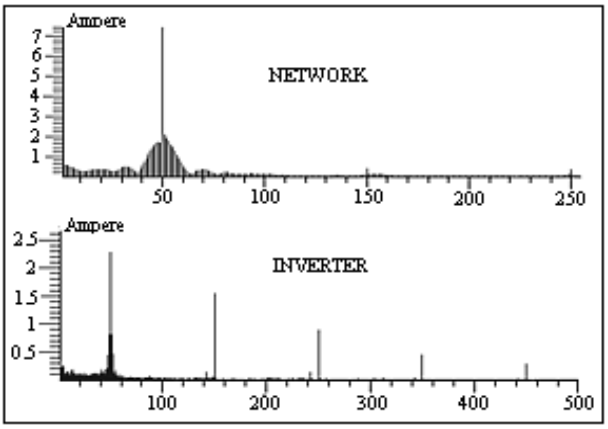

Fig. 8. Harmonic content of the supply current (network fed and inverter-fed motor).

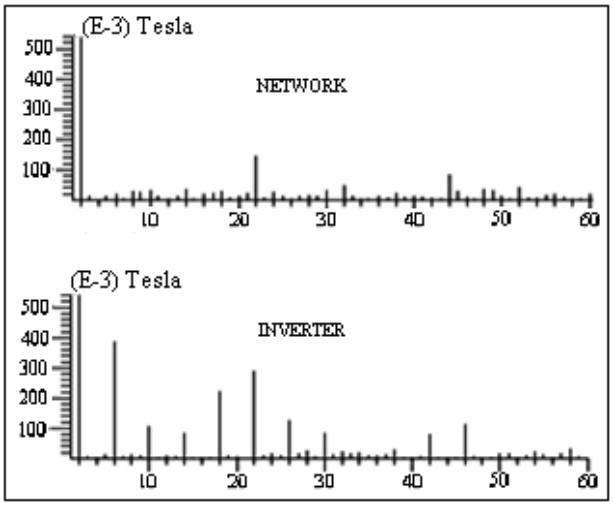

Fig. 9. Harmonic content of the air-gap flux density.

V. RESULTS AND CONCLUSIONS.

Noise measurements were performed on a 0.75 kW, 1500 rpm, 4 pole, 24 stator and 30 rotor slots, motor fitted with several capacitor values: 36 uF (standard value), 30 uF , 50 uF. The measurements were performed in a semi-anechoic chamber according to the ISO 1680/1 standard. The motor was supplied in turn by the network and by a power supply inverter produced by "Invertek" England.

The specific noise-frequency level diagrams have been traced under the following conditions:

1. U = 230 V, f = 50 Hz, no load, network supply;
2. U = 230 V, f = 50 Hz, no load, inverter supply, 4 kHz switching frequency.

The noise of induction motors is produced by the vibration of the motor components. The magnetic noise component is generated by the electromagnetic forces acting on the stator core. In the case of the inverter-fed motor the frequencies of these forces can be estimated using expressions (15), (16), (17), (18) and (19).

Figure 10 and Figure 11 show the measured noise-frequency level diagrams for the network-fed and inverter-fed induction motor. As it can be seen by comparison, the magnetic component of noise is modified when working with inverter-fed motors. As predicted by applying expressions (14) and (15), new noise peaks appear for the inverter fed motor in the frequency range around the inverter switching frequency, 4 kHz.

In order to clearly illustrate the effects of the supply as well as that of the capacitor value, on the noise level of the tested motor, Table I shows a comparison between results obtained for the same motor fitted with different capacitor values.

TABLE I
COMPARISON OF THE NOISE LEVEL FOR NETWORK AND INVERTER-FED MOTOR WITH DIFFERENT CAPACITOR VALUES

Capacitor value [uF]	Noise level of network-fed motor [dB]:	Noise level of inverter-fed motor [dB]:
30	52.3	61
36	52.7	62.1
50	53.9	64.6

Several conclusions may be drawn:

1. The inverter-supply causes a drastic increase of the noise levels by more that 10 dB, as compared to the case of the network supplied motor.
2. For the network-fed motor, the noise level is increased as the value of the running capacitor is increased.

The same motor was modelled using the finite elements software Cedrat Flux 2D/3D. Figure 12 shows the computed waveform of the magnetic force exerted on the stator, for the network-fed motor fitted with a 36 uF capacitor.

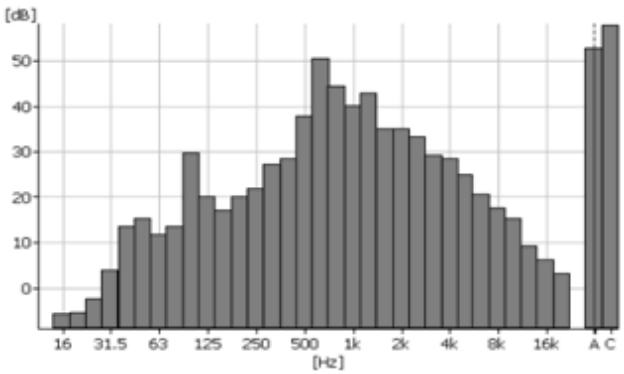

Fig. 10. No load, standard 36 uF capacitor, network supply.

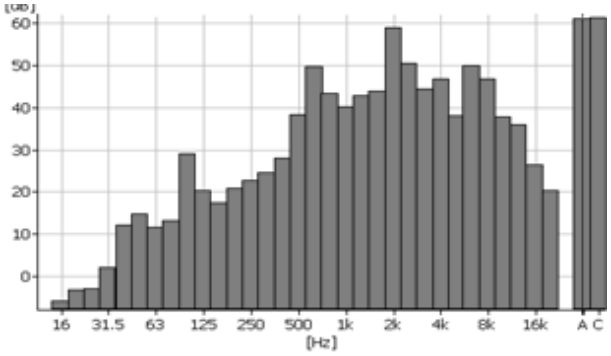

Fig. 11. No load, standard 36 uF capacitor, inverter supply, 4 kHz switching frequency.

The computation relies on the Maxwell Stress method taking into account only the normal component of the flux density. Figure 13 shows the magnetic force spectrum in the case of network and inverter-fed motor. The influence of the inverter supply on the force spectrum is shown. New harmonics predicted by expressions (13) appear in the spectrum, around the 4 kHz frequency.

Table II shows a comparison between the magnetic force levels obtained for the network fed and inverter fed motor, in the case of different capacitor values. When comparing the magnetic force levels for the case of the network-fed and inverter-fed motor it can be noted that the magnetic force level is lower for the inverter case. This is because the no load current for the network fed motor is much larger than that of the inverter fed one. This in turn affects the amplitude of the air-gap flux density. In both cases, the amplitude of the magnetic force increases as the value of the capacitor is increased.

TABLE II
COMPARISON OF THE MAGNETIC FORCE LEVEL FOR NETWORK AND INVERTER-FED MOTOR WITH DIFFERENT CAPACITOR VALUES

Capacitor value [uF]	Magnetic force level for the network-fed motor [N]:	Magnetic force level for the inverter-fed motor [N]:
30	0.87	0.52
36	1	0.6
50	1.34	1

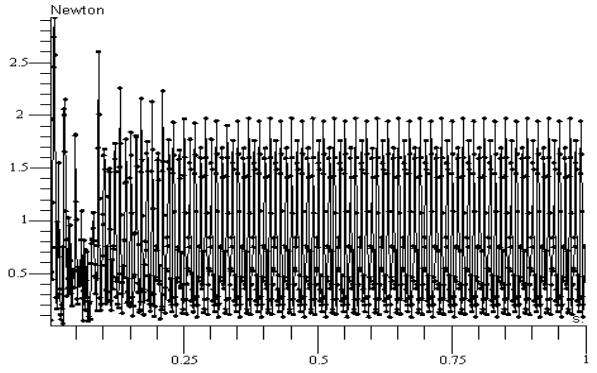

Fig. 12. Magnetic force exerted on the stator of the network fed motor. fitted with a 36 uF capacitor.

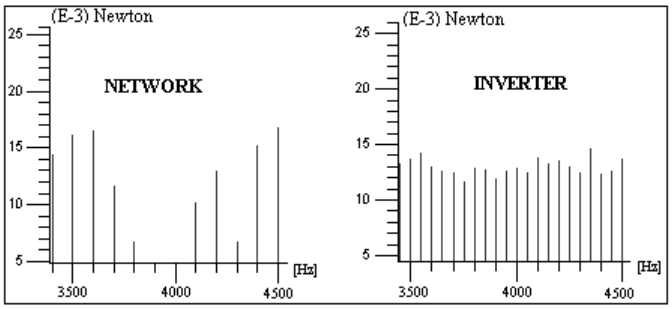

Fig. 13. Magnetic force spectrum comparison for the network and inverter-fed motor fitted with a 36 uF capacitor.

The increased harmonic content of the supply current for the inverter supply leads to an increased possibility of matching the magnetic force frequencies with the natural stator core frequency leading to resonance and an increased noise level, which explains the results presented in Table 1.

ACKNOWLEDGMENT

This paper is supported by the Sectoral Operational Programme Human Resources Development (SOP HRD), ID59321 financed from the European Social Fund and by the Romanian Government."

REFERENCES

[1] K.C. Maliti, "Modelling and Analysis of Magnetic Noise in Squirrel-Cage Induction Motors", Ph.D. dissertation, Stockholm Royal Institute of Technology, 2000

[2] P.C. Krause, O. Wasynczuck, S.D. Sudhoff, *Analysis of Electric Machinery*, Piscataway, New Jersey, IEEE Press, 1996.

[3] I. Boldea, S.A. Nassar, *The induction machines handbook - Second Edition*, CRC Press, 2009.

[4] F. Blaabjerg, F. Lungeanu, K. Skaig, M. Tommes, "Two-phase induction motor drives", in 2004 IEEE Industry Applications Magazine, Issue 4, pp. 24-32.

[5] J. Gieras, C. Wang, J. Cho Lai, *Noise of polyphase electric motors*, Taylor&Francis, 2006

[6] I. Boldea, S.A. Nassar, *The induction machine handbook*, CRC Press, 2002.

[7] B. Malcom, *Practical Variable Speed Drives and Power Electronics*, Newnes, Oxford, 2003.

[8] J. Besnerais, "Reduction of Magnetic Noise in PWM supplied induction machines", Ph.D. dissertation, Laboratoire d' Electricite et d'Electronique de Puissance d'Ecole Centrale de Lille, 2008

[9] S. Garcia Otero, M. Devaney, "Minimization of acoustic noise in variable speed induction motors using a modified PWM drive", IEEE Trans on IA, Vol. 30 (1), pp. 111-115, 1994.